Journal of
Ceramic Science
and Technology

J. Ceram. Sci. Tech., 02 [03] 179-182 (2011)
DOI: 10.4416/JCST2011-00014
available online at: http://www.ceramic-science.com

Heat Transfer in Transparent YAG Nanoceramic

J. Mucha[1], A. Chuchmała[*2, 3], D. Hreniak[1], A. Jeżowski[1] and W. Strek[1]

[1]Institute of Low Temperature and Structure Research, Polish Academy of Sciences, P.O. Box 1410, 50 – 950 Wroclaw, Poland;
[2]Institute of Electrical Engineering Fundamentals (I7), Wroclaw University of Technology, Wybrzeze Wyspianskiego 27, 50 – 370 Wroclaw, Poland;
[3]Electrotechnical Institute, Division of Electrotechnology and Materials Science, M. Sklodowskiej-Curie 55/61, 50 – 369 Wroclaw, Poland

received March 19, 2011; received in revised form May 6, 2011; accepted June 7, 2011

Abstract

Thermal conductivity in transparent YAG nanoceramic was measured with the LTHP method in the temperature range 4 – 300 K. It was found that the thermal conductivity of nanoceramics with an average grains size of 16 nm was much lower compared to YAG crystal and polycrystalline ceramics composed of micro-size grains. The results were discussed in terms of the Kapitza resistance model. At about 200 K, Kapitza resistance becomes negative, which indicates a connection with apparent negative thermal conductivity.

Keywords: Ceramics, amorphous materials, nanostructures, thermal conductivity, YAG

I. Introduction

The thermal conductivity of optically active materials is an important factor that determines the conditions of their application in optoelectronics, especially in high-power lasers. The principal question is the relationship between the structure and morphology of the crystals or ceramics and their thermal conductivity. Interesting studies of heat transport in polycrystalline materials have been conducted recently. These concern the influence of crystal grain sizes and grain boundaries [1–3] on phonon scattering, which has a significant impact on heat transport. We recently reported on the effect of crystallite size on the thermal conductivity of $BaTiO_3$ nanoceramics composed of grains with average sizes 30 – 100 nm [4].

YAG crystal is a material characterized by relatively high thermal conductivity and excellent thermal stability [5]. Because of its optical properties it is widely used as a lasing medium in solid-state lasers. However, the relatively high costs of good quality crystals prompted the development of an alternative production method, which has led to the application of YAG ceramics [6]. These are characterized by much lower production costs, improved possibilities for composition control and ease of fabrication [7–9]. Compared to single crystals, ceramics exhibit far inferior heat transfer owing to the blocking effect of grain boundaries. In addition, thanks to their stability, YAG ceramics could find application as thermal barrier coatings [10], along with other materials with low thermal conductivity such as yttria-stabilized zirconia [11] or mullite [12].

In this present work we report on our studies of thermal conductivity in transparent YAG nanoceramics.The mechanisms responsible for phonon scattering processes are discussed in terms of the Kapitza resistance model.

* Corresponding author: chuchmala@iel.wroc.pl

II. Experimental

(1) Material preparation

Starting YAG material was prepared with the modified Pechini method [13]. Stoichiometric amounts of yttrium nitrate (99.99 %) and aluminium nitrate (99.99 %) were dissolved in an aqueous citric acid and ethylene glycol solution to give the appropriate molar ratio 3:5:16:6.5 respectively. The reactants solution was then ultrasonically stirred for 2 h and placed into a dryer for three days at 110 °C. The brown polyester resins obtained were heat-treated at 900 °C in an electric oven in air for 16 h. The nanoceramic was formed by low-temperature high-pressure sintering at 8 GPa and 450 °C [14].

(2) XRD and thermal conductivity measurements

XRD measurements were performed with an X'Pert PRO Diffractometer in 2θ range 10 – 110°. The XRD patterns for the starting powder and sintered ceramics are presented in Fig. 1. In the case of the starting powder there are unidentified peaks (denoted by *), which, however, disap pear after the sintering process. They probably come from the additional phases such as oxides of yttrium or aluminium. The Scherrer formula [15] applied to the peak at 2θ = 20° gives the values for the average grain diameter of the nanopowder and nanoceramics as 21 and 16 nm respectively.

The thermal conductivity was measured with the stationary heat flux method in the temperature range 4 – 300 K. The experimental setup and the measurement procedure

have been described in detail previously [16, 17]. The temperature gradient along the sample was in the range 0.1 – 0.5 K. Particular care was taken to avoid parasitic heat transfer between the sample and its environment. The measurement error was below 2 % and the surplus error estimated from the scatter in the measurement points did not exceed 0.3 %.

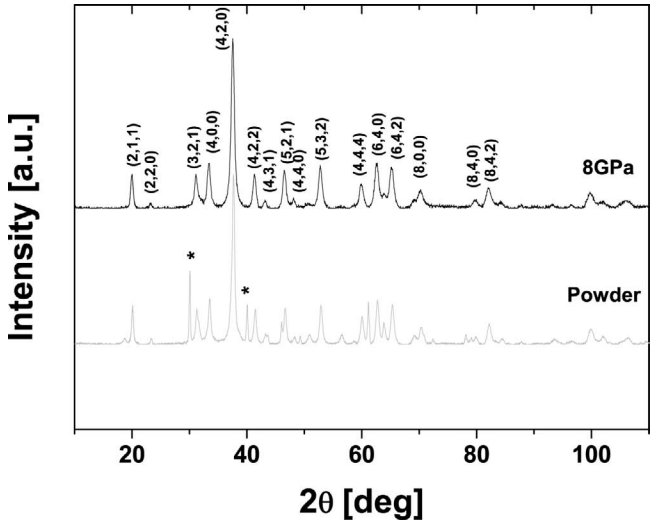

Fig. 1: XRD patterns for YAG starting powder and nanoceramics.

where ΔT is the temperature discontinuity at the interface and σ_K is the Kapitza conductance. For grained materials, composed of nanocrystallites, heat flow is impeded by the grain boundaries because phonon scattering occurs. The Kapitza resistance, $R_K = 1/\sigma_K$, describes the resistance of heat transport owing to interfaces between the grains. An illustrative temperature profile of nanoceramics is presented in Fig. 3.

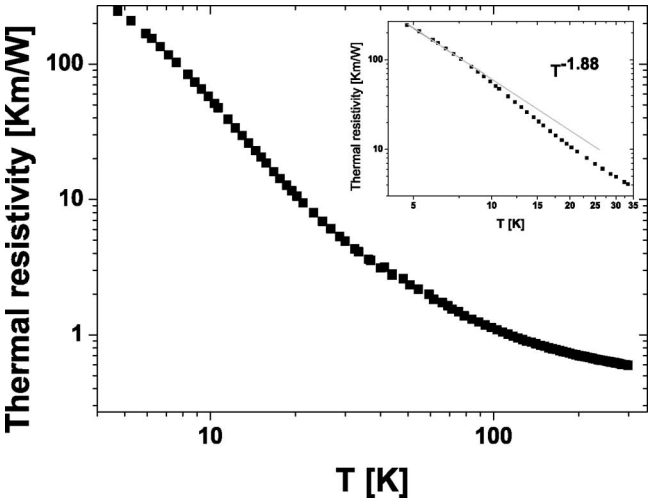

Fig. 2: The temperature dependence of the thermal resistivity of YAG nanoceramics.

III. Results and Discussion

As stated earlier, during sintering under pressure, the grains shrink substantially. This indicates a core-shell type of structure formation in which the crystalline core is wrapped in an amorphous shell [18]. Amorphous bodies are characterized by a plateau for thermal resistivity, *W(T)*, dependence at approx. 10 K. Below this value, *W(T)* should exhibit proportionality to T^{-2}. The mechanisms responsible for such behaviour are well described in the literature, for example in a monograph [19]. It is interesting to note that only few materials exhibit behaviour typical for amorphous solids: the plateau is weakly visible and often occurs at higher temperatures.

The temperature dependence of *W(T)* is presented in Fig. 2. As can be seen in the inset, for low temperatures $W(T) \sim T^{-1.88}$, which is very close to T^{-2}. This is in good agreement with the statement above and it could be concluded that the fitting to a straight line is rather good up to about 10 K. However, the plateau expected at this temperature is shifted towards approx. 300 K.

In nanoceramics with grains size approaching a few nm in scale, heat transport is governed by the Kapitza resistance [20], introduced initially for the interface between liquid helium and solid medium. It was shown that it could be applicable even at room temperature in analysis of the thermal conductivity of polycrystalline materials [21].

The Kapitza resistance model is based on a concept of temperature discontinuity at an interface between two bodies (particles, grains). As a result, the thermal current *J* may be expressed, from the definition, with a simple formula:

$$J = \sigma_k \Delta T, \qquad (1)$$

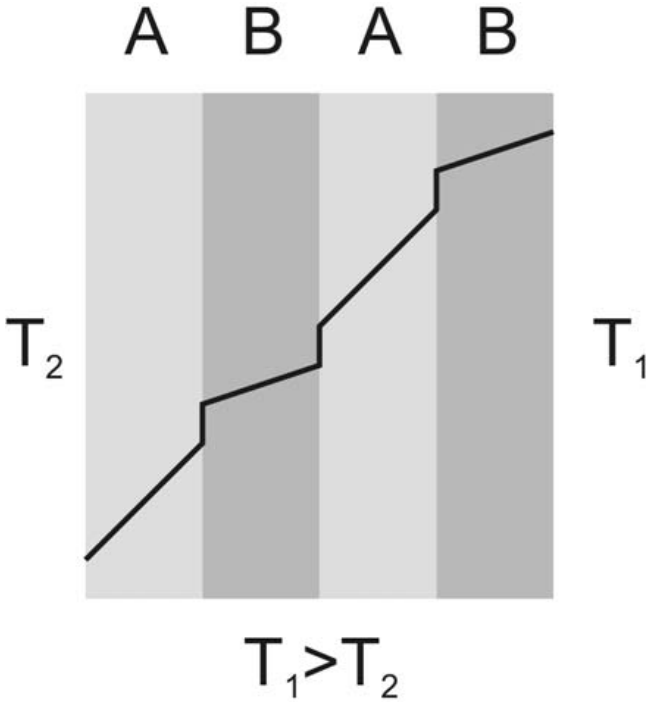

Fig. 3: The temperature profile for material with alternating layers of different heat conductivity. The slope of temperature change in each layer corresponds to its thermal conductivity (temperature T_1 is at the hot side of sample, T_2 is at the cold side).

Grain boundaries impede heat transport and cause a drop in temperature across the boundary. This drop is dependent on the transmission coefficient for phonons. Owing to the very small grain size (of the order of 10s nanometres), the drop across a single grain could be approximated

with a linear function. This gives us the formula connecting the Kapitza resistance with the thermal resistivity [22]:

$$\frac{W_0(T)}{W(T)} = \left(1 + \frac{R_K(T)}{dW_0(T)}\right)^{-1}, \quad (2)$$

where $W_0(T)/(W(T))$is the thermal resistivity of a single crystal (polycrystalline material), d – the mean grain size, $R_K(T)$ – the Kapitza resistance. Because of the temperature dependence of heat resistivity, the Kapitza resistance should also be temperature-dependent.

Moreover, transmission through grain boundaries could be temperature-dependent, which may introduce a different temperature dependence than the $R_K \sim T^{-3}$ postulated by Pollack [23]. Heat transport between adjacent materials is influenced by differences in the density of each material and in the morphology between the materials.

In order to determine $R_K(T)$ from Eq. 2, we need to know the temperature dependence of the thermal resistivity of a YAG single crystal. This could be obtained with the Callaway model [24], which was found to be in good agreement with the experimental data for single crystal samples as pointed out by Numazawa *et al.* [25]. In the Callaway model the thermal conductivity may be expressed as:

$$\kappa = \frac{k_B}{2\pi^2 v}\left(\frac{k_B T}{\hbar}\right)^3 \int_0^{\theta_D/T} \frac{x^4 e^x}{(e^x - 1)^2}\tau dx, \quad (3)$$

with v as phonon velocity, τ - the relaxation time of phonons, $x = \hbar\omega/k_B T$, θ_D – Debye temperature and $\hbar$ – Dirac constant . In general, the relaxation speed τ^{-1} could be written as a sum of contributions from different scattering mechanisms:

$$\tau^{-1} = \tau_I^{-1} + \tau_b^{-1} + \tau_U^{-1}\ \tau_N^{-1}, \quad (4)$$

where I, b, U and N denote the scattering on impurities, grain boundaries, Umklapp processes and the normal process respectively. Temperature dependence of the overall relaxation speed could be written in explicit form as:

$$\tau^{-1} = B_I\omega^4 + \frac{v}{L} + B_U\omega^2 T^3 \exp\left(-\frac{\Theta_D}{2T}\right) + B_N\omega^3 T^3, \quad (5)$$

where B_I, v, L, B_U and B_N are fitting parameters. In our calculations we used the values: $B_I = 1.46 \times 10^{-44}\ s^3$, $v = 5000\ m/s$, $L = 7.326 \times 10^{-4}\ m$, $B_U = 40.722 \times 10^{-22}\ s/K^3$, $B_N = 5.8 \times 10^{-36}\ s^2/K^3$, as in [25]. This function allows us to determine the temperature dependence of the Kapitza resistance for the sample under investigation. Writing R_K in explicit form we obtain:

$$R_K(T) = d(W(T) - W_0(T)). \quad (6)$$

Solving Eq. 3 numerically and taking $d = 16$ nm as determined from the XRD pattern analysis, the temperature dependence of R_K could be obtained, as shown in Fig. 4. Moreover, the values of $W(T)$ are higher for the nanoceramics sample than for the single crystal or micrometre grain ceramics, which can be seen from the graph (Fig. 6) in [25], where the values of thermal conductivity are in the range of 0.06 to 8 W/cmK (dependent on sample). These values correspond to values for $W(T)$ of 0.17 to 0.0125 Km/W respectively. This is significantly lower than in the case of nanoceramics, for which $W(T)$ attains values in the range 0.6 to above 200 Km/W. Similarly, the values of thermal conductivity for crystals reported by Sato *et al.* (Fig. 1 in [26]) attains values of 9 – 10 W/mK at 25 °C, which corresponds to a thermal resistivity of 0.1 – 0.11 Km/W, significantly lower than 0.6 at approx. 300 K reported in this work.

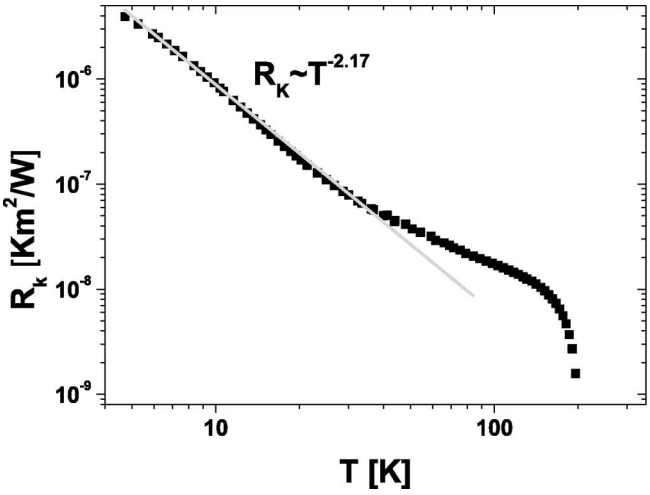

Fig. 4: Temperature dependence of the Kapitza resistance for YAG nanoceramics.

The $R_K(T)$ plot needs closer analysis. At the lowest temperatures, the $R_K \sim T^{-2.17}$, which is substantially different from the T^{-3} dependence as mentioned above. This could reflect the fact that the temperature profile at grain boundaries contains two steps because of the presence of amorphous phase. Secondly, as it could be seen from above plot, R_K drops rapidly above about 150 K and becomes negative above about 200 K. The origin of such behaviour is unclear at the present stage of investigation. It can be seen (Fig. 2) that at 200 K the region of plateau emerges in $W(T)$ vs. T. From Eq. 6, it is easy to see that negative values of R_K originate in the thermal resistivity of the crystal exceeding the thermal resistivity of the ceramic sample. Because the Kapitza resistance describes only the heat transfer across, but not parallel to, grain boundaries, heat flow between two grains parallel to the boundary could have a significant influence on the R_K values, which is not taken into account in Eq. 2. To obtain a deeper understanding of this behaviour, more sophisticated investigations are planned.

IV. Conclusions

The thermal transport properties of YAG nanoceramics prepared with the LTHP method have been investigated. XRD analysis indicates shrinkage of the grains, implying the formation of amorphous phase enveloping the crystalline particles. The thermal resistivity, W, measurements indicate that heat transport is impeded by the amorphous part of the sample. At low temperatures, $W(T) \sim T^{-1.88}$, which is close to theoretical proportionality to T^{-2}. However the plateau, which should occur at about 10 K, is shifted towards higher temperatures and starts to form near the upper limit of the measured temperatures (300 K). W attains values significantly larger than in the case of the single crystal or microcrystalline ceramics reported by Numazawa *et al.* [25] and Sato *et al.* [26] Analysis of experimental results in terms of Kapitza resistance, R_K, indicates

$R_K(T) \sim T^{-2.17}$ at a low temperature regime, which suggests the dependence of the transmission coefficient between grains on temperature. Moreover, it exhibits a substantial drop above approx. 150 K, which in effect leads to negative values. At the present stage of investigations, the nature of such behaviour is not clear and requires further investigation.

Acknowledgements

The authors would like to thank Prof. W. Łojkowski for permitting access to the pressing equipment.

References

1 Klemens, P.G.: Thermal resistance due to grain boundaries. In: Thermal Conductivity, 21, Edited by Cremers C. J. and Fine H. A., Plenum Press, New York, USA, (1990).

2 Salamon, M.B., Jaime, M.: The physics of manganites: Structure and transport, *Rev. Mod. Phys.*, **73**, 583 – 628, (2001).

3 Watari, K., Nakano, H., Sato, K., Urabe, K., Ishizaki, K., Cao, S., Mori, K.: Effect of grain boundaries on thermal conductivity of silicon carbide ceramic at 5 to 1300 K, *J. Am. Ceram. Soc.,* **86**, 1812 – 1814, (2003).

4 Jezowski, A., Mucha, J., Pazik, R., Strek, W.: Influence of crystallite size on the thermal conductivity in $BaTiO_3$ nanoceramics, *Appl. Phys. Lett.*, **90**, 114104, (2007).

5 Kaminskii, A.A.: Laser crystals, Springer, Berlin, Heidelberg, New York, (1981).

6 Ikesue, A., Furusato, I., Kamata, K.: Fabrication of polycrystal line, transparent YAG ceramics by a solid-state reaction method, *J. Am. Ceram. Soc.*, **78**, 225 – 228, (1995).

7 Lu, J., Prahu, M., Xu, J., Ueda, K., Yagi, H., Yanagitani, T., Kaminskii, A.A.: Highly efficient 2 % Nd:Yttrium aluminum garnet ceramic laser, *Appl. Phys. Lett.*, **77**, 3707 – 3709, (2000).

8 Lu, J., Murai, T., Takaichi, K., Uematsu, T., Misawa, K., Prabhu, M., Xu, J., Ueda, K., Yagi, H., Yanagitani, T., Kaminskii, A.A., Kudryashov, A.: 72 W Nd:$Y_3Al_5O_{12}$ ceramic laser; *Appl. Phys. Lett.*, **78**, 3586 – 3588, (2001).

9 Yagi, H., Yanagitani, T., Takaichi, K., Ueda, K., Kaminskii, A.A.: Characterizations and laser performances of highly transparent Nd^{3+}:$Y_3Al_5O_{12}$ laser ceramics, *Opt. Mater.*, **29**, 1258 – 1262, (2007).

10 Nitin, P.P., Klemens, P.G.: Low thermal conductivity in garnets, *J. Am. Ceram. Soc.*, **80**, 1018 – 1020, (1997).

11 Samsonov, G.V.: The Oxide Handbook, 2nd edition., IFI/ Plenum, New York, (1982).

12 Lackey, W.J., Stinton, D.P., Cerny, G.A., Schaffhauser, A.C., Fehrenbacher, L.L.: Ceramic coatings for advanced heat Engines – a review and projection, *Adv. Ceram. Mater.*, **2**, 24 – 30, (1987).

13 Pechini, M.P.: Method of preparing lead and alkaline earth titanates and niobates and coating method using the same to form a capacitor, US Patent 3 330 697, (1967).

14 Fedyk, R., Hreniak, D., Łojkowski, W., Strek, W., Matysiak, H., Grzanka, E., Gierlotka, S., Mazur, P.: Method of preparation and structural properties of transparent YAG nanoceramics, *Opt. Mat.*, **29**, 1252 – 1257, (2007).

15 Scherrer, P., Göttinger Nachrichten Gesell. **2**, 98 – 100, (1918).

16 Jezowski, A., Mucha, J., Pompe, G.: Thermal conductivity of the amorphous alloy $Fe_{40}Ni_{40}P_{14}B_6$ between 80 and 300 K, *J. Phys. D: Appl. Phys.*, **20**, 1500 – 1506, (1987).

17 Mucha, J., Dorbolo, S., Bougrine, H., Durczewski, K., Ausloos, M.: Analysis of experimental conditions for simultaneous measurements of transport and magnetotransport coefficients of high temperature superconductors, *Cryogenics*, **44**, 145 – 149, (2004).

18 Lukowiak, A., Wiglusz, R.J., Maczka, M., Gluchowski, P., Strek, W.: IR and raman spectroscopy study of YAG nanoceramics, *Chem. Phys. Lett.*, **494**, 279 – 283, (2010).

19 Amorphous Solids, Low-Temperature Properties, edited by Phillips, W.A., Springer Verlag Berlin, Heidelberg, New York (1981).

20 P.L. Kapitza, Zh. Eksp. Teor. Fiz. 11 (1941) 1 [English transl.: *J. Phys. U.S.S.R.* 4 (1941) 181].

21 Nan, C.W., Birringer, R.: Determining the kapitza resistance and the thermal Conductivity of Polycrystals: A simple model, *Phys. Rev. B*, **57**, 8264 – 8268, (1998).

22 Yang, H.S., Bai, G.R., Thompson, L.J., Eastman, J.A.: Interfacial thermal resistance in nanocrystalline yttria-stabilized zirconia, *Acta Mater.*, **50**, 2309 – 2317, (2002).

23 Pollack G. L.: Kapitza resistance, *Rev. Mod. Phys.,* **41**, 48 – 81, (1969)

24 Callaway, J.: Model for lattice thermal conductivity at low temperatures, *Phys. Rev.*, **113**, 1046 – 1051, (1959).

25 Numazawa, T., Arai, O., Hu, Q., Noda, T.: Thermal conductivity measurements for evaluation of crystal perfection at low temperatures, *Meas. Sci. Technol.*, **12**, 2089 – 2094, (2001).

26 Sato, Y., Akiyama, J., Taira, T.: Effects of rare-earth doping on thermal conductivity in $Y_3Al_5O_{12}$ crystals, *Opt. Mater.*, **31**, 720 – 724, (2009).